Advances in Geo-Energy Research

Vol. 6, No. 4, p. 276-285, 2022

Original article

# Improving recovery efficiency by $CO_2$ injection at late stage of steam assisted gravity drainage

Hengyuan Gong[1], Chunsheng Yu[1]*, Qi Jiang[1], Na Su[2], Xiao Zhao[1], Zhaoqi Fan[3]

[1] *School of Petroleum and Natural Gas Engineering, Southwest Petroleum University, Chengdu 610500, P. R. China*

[2] *SINOPEC Southwest Oil & Gas Company, Chengdu 610500, P. R. China*

[3] *Chemical and Natural Gas Engineering, Texas A&M University-Kingsville, TX 78363, United States*

**Keywords:**
Heavy oil reservoir
SAGD wind-down
$CO_2$ displacement
enhanced oil recovery
$CO_2$ storage

**Cited as:**
Gong, H., Yu, C., Jiang, Q., Su, N., Zhao, X., Fan, Z. Improving recovery efficiency by $CO_2$ injection at late stage of steam assisted gravity drainage. Advances in Geo-Energy Research, 2022, 6(4): 276-285.
https://doi.org/10.46690/ager.2022.04.02

**Abstract:**
The high recovery performance of steam-assisted gravity drainage (SAGD) makes it a popular option for heavy oil resources. Currently, most of the heavy oil reservoirs developed by SAGD in China are in the late development phase, with high energy consumption due to reduced thermal efficiency. The use of SAGD wind-down processes involving $CO_2$ in combination with steam for heavy oil recovery is considered as a viable alternative to limit energy consumption, and also reduce the amount of greenhouse gas emissions by leaving $CO_2$ behind in the reservoir. Study reveals that the dissolution and demulsification of $CO_2$ in crude oil can reduce the viscosity of emulsified heavy oil by more than 50%. When the steam chamber temperature reaches 200 °C, the amount of solid phase deposition induced by $CO_2$ extraction is only 0.016 kg/m$^3$, the rock wettability changes from lipophilic to hydrophilic, and the higher the reservoir temperature, the stronger the hydrophilicity is, which reduces the adhesion power of the oil phase and facilitates the stripping of crude oil from the rock surface. Numerical simulation studies have been carried out utilizing STARS to obtain energy efficient utilization and improved steam chamber characteristics. Heat loss from SAGD baseline is 1.77 times that with $CO_2$ injection process, but the recovery factor is only 2.48% higher. At the initial stage with $CO_2$ injection, the steam chamber continues its lateral expanding, which increases the recovery factor at the initial stage of $CO_2$ injection by about 6%. One year after $CO_2$ injection, gas channeling results in lower recovery than traditional SAGD process, and 38.4% of the injected $CO_2$ is stored in the reservoir from this study.

## 1. Introduction

Steam assisted gravity drainage (SAGD) (Butler and Stephens, 1981) is a mature technology for the development of heavy oil reservoirs and has been applied industrially at a large scale in China and abroad. Under the SAGD process, on the one hand, traditional SAGD process requires high quality steam overlap makes the steam chamber develop rapidly upward, when steam chamber reaches the top of the reservoir, resulting in significant thermal energy loss to overburden layer; On the other hand, due to the heterogeneity of the reservoir, the expansion of the steam chamber is extremely uneven, which reduces the sweep volume of steam, resulting in reduced oil recovery factor. In addition, the high water cut in the produced fluid in the later stage of SAGD process, increasing the cost of operation and other issues. Now, a lot of research has been done to improve energy efficiency for SAGD process.

In 1999, Butler proposed steam and gas push (SAGP) to improve thermal efficiency of SAGD technology (Butler, 1999), by injecting non-condensable gas ($CO_2$, $CH_4$, $N_2$, etc.) or co-injection with steam to lower the average temperature of the steam chamber and reduce the heat loss to the overburden layer. Experimental studies indicate that non-condensable gas could be significantly improved the steam-oil ratio (Gu et al., 2013; Mohammad, 2022). Different strategies for SAGD wind-down process are proposed (Ali et al., 2008) to effectively

*Corresponding author.
*E-mail address*: ghy257248@163.com (H. Gong); yuchunsheng_2000@163.com (C. Yu); qijiang@shaw.ca (Q. Jiang); angela.sue@163.com (N. Su); zxccyyfj@163.com (X. Zhao); zhaoqi.fan@tamuk.edu (Z. Fan).
Yandy Scientific Press
2207-9963 
Received April 2, 2022; revised April 29, 2022; accepted May 5, 2022; available online May 8, 2022.

utilization of remaining pressure and thermal energy in the reservoir. When 3/4 of the reservoir is heated, with deteriorating instantaneous oil-steam ratio, the continuous injection of pure steam at this stage may become uneconomic. Injection of non-condensable gas (especially $CO_2$ gas) can be more efficient by making better use of the remaining energy from the reservoir to continue production and increase oil recovery factor (Ren et al., 2020). At present, it is urgent to study the start-up timing and injection volume of non-condensable gas from experimentally and theoretically.

Under high temperature and pressure, the physical and chemical interactions between $CO_2$ and heavy oil can be primarily characterized by dissolution and expansion of gas, energy increase, dissolution and viscosity reduction; demulsification and viscosity reduction; extraction light hydrocarbons; lowering interfacial tensions; alteration of rock wettability; dissolved gas flooding; enhanced oil drainage rate, etc. (Zhang et al., 2014; Dong et al., 2019). Davarpanah and Mirshekari (2020) studied the effects of dissolving ability of $CO_2$ on oil recovery, crude oil density and viscosity, and showed that dissolved $CO_2$ can slightly reduce the viscosity and density of crude oil and improve oil recovery. But in the low pressure (1–4 MPa), the enhanced oil recovery rate after dissolving $CO_2$ is basically unchanged. Wang et al. (2020) used high-pressure visualization experimental equipment to study the diffusion capacity of $CO_2$ in heavy oil. With the pressure increased by 1.8 MPa, the diffusion coefficient significantly increased from $6.198\times10^{-9}$ to $25.333\times10^{-9}$ $m^2/s$, effectively improve the solubility of $CO_2$.

Zhao et al. (2005) uses 2-D physical model, studying on the performance of injection $N_2$ in the SAGD wind-down stage. After $N_2$ injection, additional 12.5% of the original oil-in-place (OOIP) is recovered, with temperature at the steam chamber interface is still rising slightly at the initial stage with $N_2$ injection. Li et al. (2019) proposed an optimal volume ratio of $N_2$ to steam at 8:2 for $N_2$-assisted SAGD process using the two-dimensional SAGD visualization model. Under this ratio, the expanded swept volume is 8.9% and the recovery factor is 49.12%. Ehsan et al. (2019) used a large-scale three-dimensional SAGD physical model to study the feasibility of air-assisted SAGD. Results showed that air-assisted SAGD could not only reduce the steam-oil ratio, but also maintain the steam chamber pressure, resulting in increased SAGD recovery factor. Xi et al. (2019) research results show that $CO_2$-assisted steam flooding can effectively expand the lateral swept volume of the steam chamber, reducing steam partial pressure and heat loss, increasing the oil-steam ratio by 34%, and the recovery factor by 5.4%.

Researchers have carried out a large number of numerical simulation studies with the injection non-condensable gas in the later stage of SAGD. Zhao et al. (2003) carried out experiments and numerical simulation runs to study a gas injection SAGD wind-down process, show that the feasibility of injecting non-condensable gas in the SAGD wind-down stage based on the results from numerical simulation. Zhang et al. (2014) performed the analysis on the feasibility of $CO_2$ assisted SAGD process, it is believed that the injected non-condensable gas can effectively expand the lateral expansion of the steam chamber and prolong the SAGD production time by 3–4 years. Ali et al. (2008) made comparison on the oil recovery of $CO_2$ injection in different periods of SAGD, it is believed that with $CO_2$ injection in the late stage of SAGD could achieve the similar recovery factor as traditional SAGD. Wang et al. (2017) reveals that $CO_2$-assisted SAGD production at the reservoir temperature of about 200 °C can effectively improve the SAGD recovery factor. In the context of carbon neutrality, as the oil displacement medium, $CO_2$ can achieve the effect of reducing carbon emissions. Therefore, the comprehensive analysis believes that $CO_2$ is the first choice for non-condensable gas injection in the late stage of SAGD development.

This paper firstly studies the interaction mechanism between heavy oil and $CO_2$ under different pressure, temperature and water saturation conditions. Secondly, the high temperature and pressure automatic interfacial tension meter was used to measure the wettability of the rock surface under different temperature, pressure and reaction times. Finally, a numerical simulation study was carried out using STARS, and a dual horizontal well SAGD model was established to study the effect of $CO_2$ injection on the steam chamber development characteristics, energy utilization efficiency and oil production rate.

## 2. The experiment

### 2.1 Crude oil properties and emulsification

The crude oil samples selected for this study are taken from well PX-2 in Daqing Oilfield. The oil density is 931.5 $kg/m^3$ at 20 °C and its viscosity is 10,900 mPa·s, which is classified as extra-heavy oil. The properties of crude oil are shown in Table 1. The content of resins and asphaltenes reaches 13.5%, which is one of the main reasons for the high viscosity. The

**Table 1**. Crude oil properties.

| Four-components | Content (%) | Carbon number | Content (%) | Element content | Mass percentage (%) |
|---|---|---|---|---|---|
| Saturated hydrocarbon | 49.1 | $C_5$–$C_9$ | 0.241 | C | 84.83 |
| Aromatic hydrocarbon | 36.99 | $C_{10}$–$C_{19}$ | 30.184 | H | 6.94 |
| Resins | 13.15 | $C_{20}$–$C_{29}$ | 53.978 | O | 3.57 |
| Asphaltenes | 0.35 | $C_{30+}$ | 15.602 | N | 0.67 |
| | | | | S | 0.12 |

**Table 2**. Viscosity reduction rate after dissolving with $CO_2$ at different temperatures (3 MPa).

| Temperatures (°C) | Water cut (%) | Original viscosity (mPa·s) | Crude oil viscosity after issolving $CO_2$ (mPa·s) | Viscosity reduction rate (%) |
|---|---|---|---|---|
| 80 | 0 | 137 | 132–51 | 3.6–62.8 |
| | 5 | 168 | 158–64 | 6–61.9 |
| | 10 | 207 | 165–78 | 20.3–62.3 |
| 160 | 0 | 30 | 13–29 | 3.3–56.7 |
| | 5 | 43 | 21–39 | 9.3–51.2 |
| | 10 | 55 | 26–51 | 7.3–52.7 |

carbon number in crude oil is mainly concentrated in the range of $C_{20}$–$C_{29}$ long-chain heavy carbon alkanes, consisting of 54%, and the $C_{30+}$ (ultra-heavy carbon) content is more than 15%. Entanglement and knotting between the long chain molecules will increase the internal friction and viscosity of the crude oil (He et al., 2020a). The H/C (hydrogen to carbon ratio) of crude oil is 0.0819, content of oxygen and nitrogen elements is 4.24%, indicating that the crude oil contains unsaturated alkanes and aromatic ring compounds with high molecular weight and heteroatom. Such compounds are usually amines with heterocyclic and condensed ring, phenols and ethers, which are strongly polar compounds. The resins and asphaltenes are complexed together through hydrogen bonds and intermolecular forces of the strong polar groups, which will greatly increase the crude oil viscosity (Fan et al., 2016).

When the oil-water volume ratio is 2:1, 1:1, 1:2 and 1:3, it is found that the crude oil will be slightly emulsified and the water content of water-in-oil emulsion can be high up to 10.8%, moreover, the higher the water content, the greater the viscosity of the emulsion. The measured viscosity of the emulsions at different temperatures indicates that the viscosity of the emulsion is 1.36 times higher than that of the dehydrated crude oil.

The degree of emulsification is relatively low (He et al., 2020b), which may be due to its low acid value (0.74 mg KOH/g), resulting in low surface activity of crude oil and difficult to form water-in-oil emulsions (Fig. 1).

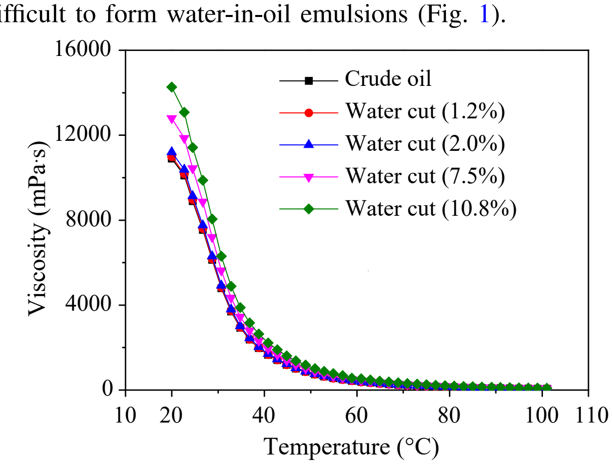


**Fig. 1**. Crude oil emulsification and viscosity increasing characteristic curve.

## 2.2 Effects of $CO_2$ on heavy oil viscosity

The effect of $CO_2$ on viscosity for heavy crude oil is much greater than that for light crude oil (Seyyed and Mehran, 2017). After the heavy oil dissolved with $CO_2$, the viscosity of the mixture is significantly reduced, which improves the mobility of the crude oil in reservoirs and mobility ratio of oil and water and the oil phase permeability (Daniel, 2021). All the above effects help to enhance the efficiency of oil recovery.

Under the 3 MPa, measure the viscosity of oil samples with different water content at 80 °C and 160 °C respectively before and after dissolving $CO_2$. Experimental results demonstrated that, when the viscosity of crude oil with dissolved $CO_2$ at 80 °C is reduced by 62.8%, 61.9%, and 62.3% respectively; under 160 °C, the viscosity will be reduced by 56.7%, 51.2%, 52.7% respectively (Table 2).

In addition, it is found that $CO_2$ has effect on the degree of demulsification. Fig. 2 shows the phase behavior of the crude oil after dissolving with $CO_2$. Only oil phase exists before pressurization (Fig. 2(a)). After dissolving with $CO_2$, the oil and water separated, indicating that $CO_2$ has the effect on dehydration and demulsification, the higher the pressure, the better the effectiveness of the demulsification (Figs. 2(b) and 2(c)). The viscosity of heavy oil emulsion will decrease after dehydration, which is beneficial to oil drainage.

## 2.3 $CO_2$ extraction and solid phase deposition

$CO_2$ has the ability to extract light hydrocarbons, which will inevitably break the balance of colloids in crude oil system and the content of heavy components increased. Under certain temperature and pressure, organic solid phases such as wax and asphaltene become easier to aggregate and flocculate, and then precipitate in the form of solid phase. Especially for heavy oil, the aggregated or precipitated solid phase blocks the pore-throats, causing the permeability of the reservoir to decrease, thereby resulting in production problems (Zanganeh et al., 2015; Song et al., 2018).

The experimental study shows that oil density is only increased by 0.23% after repeated contact between the crude oil and $CO_2$. As the number of degassing increased, the amount of solid phase deposition increased gradually. The maximum solid phase deposition amount is 0.0411 mg/ml (Fig. 4 (80 °C)), that means 1 $m^3$ of crude oil only produces less than 0.05 kg of solid phase depositions. The actual operating pressure

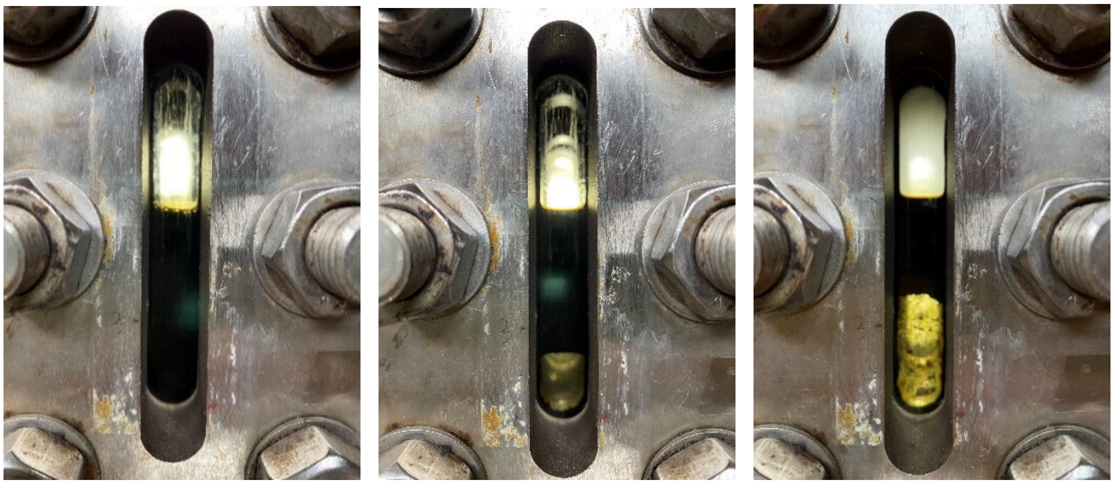

(a) 0.1 MPa, 80 °C (b) 2.4 MPa, 80 °C (c) 6.5 MPa, 80 °C

**Fig. 2**. Phase of fluid before and after $CO_2$ dissolution.

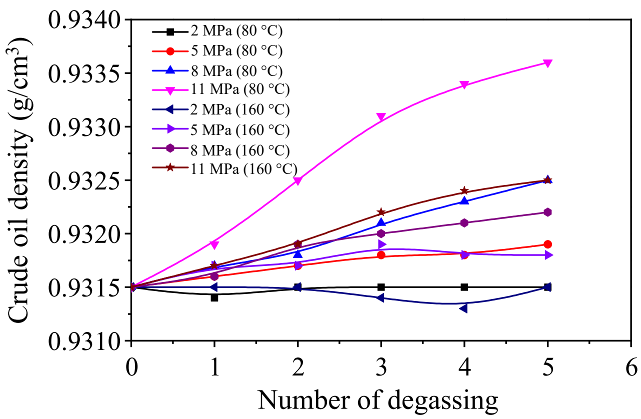


**Fig. 3**. Oil density after $CO_2$ extraction.

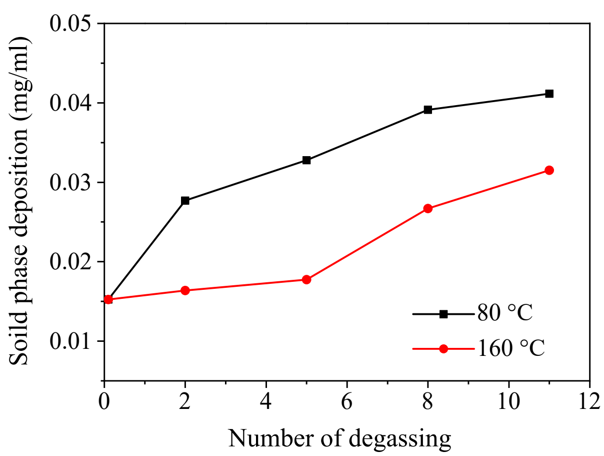


**Fig. 4**. Solid phase deposition after $CO_2$ extraction.

of SAGD steam chamber is 2–5 MPa, the solid phase deposition is expected to be less than 0.016 kg (Fig. 4 (160 °C)) per cubic meter of oil, and with the increase of temperature, there are less depositions (Figs. 3 and 4). In addition, the temperature range of aquathermolysis of heavy oil is between 200 and 350 °C. The temperature of SAGD steam chamber is about 250 °C, therefore, part of the aquathermolysis will produce $H_2$, which can also effectively inhibit the solid deposition (Hosseinpour et al., 2019).

### 2.4 $CO_2$ improves rock wettability

Heavy oil contains a lot of polar substances such as resins and asphaltenes. These substances are easily adsorbed on the rock surface during the long-term oil reservoir environment, making the rock surface lipophilic and the oil adhesion work on the rock surface greatly increased. In the oil drainage process, a large amount of remaining oil is remained in the reservoir pores in the form of oil film, which is difficult to be exploited and the oil drainage efficiency is greatly reduced. With $CO_2$ dissolved in the water forms acidic fluids, that can react with rock minerals to improve the rock surface wettability (Ameri et al., 2015; Fang et al., 2016).

The high temperature and pressure automatic interfacial tension meter was used to measure the rock surface wettability alterations under different temperature, pressure and reaction times. Experimental results show that increasing the reaction temperature and pressure, the contact angle becomes smaller, the rock hydrophilicity is enhanced, the wettability is improved (Figs. 5 and 7). When the water and rock reaction time is increased, the contact angle becomes smaller, which is conducive to the improvement of rock surface wettability (Figs. 6 and 8) and can reduce the adhesion work of the oil phase on the rock surface. It facilitates the stripping of crude oil from the rock surface.

## 3. Numerical simulation

### 3.1 Reservoir simulation model

The thermal reservoir simulator STARS developed by the CMG was used in this study. Based on the actual reservoir parameters of well PX-2 in Daqing Oilfield, a homogeneous SAGD dual horizontal well model was established. The reser-

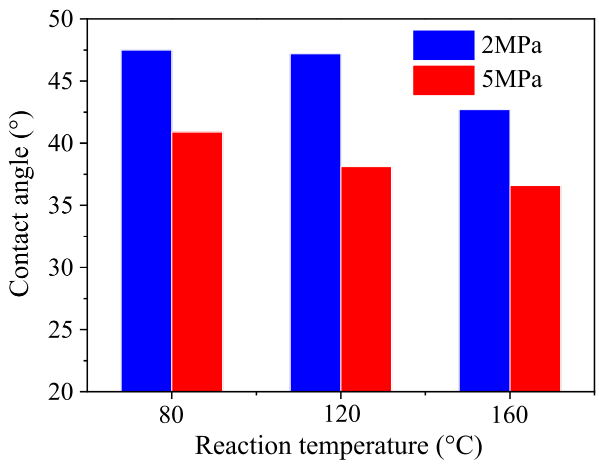


Fig. 5. Rock contact angle after water-rock reaction with different temperature and pressure.

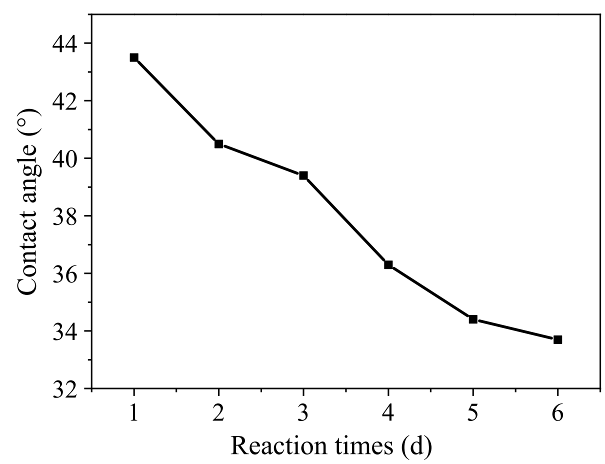


Fig. 6. Variation curve of contact angle of water-rock reaction with different reaction time.

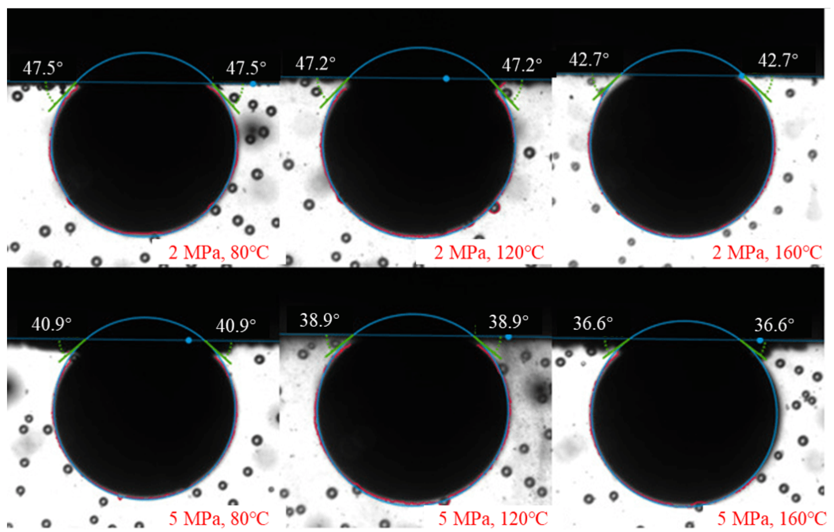


Fig. 7. Variation of rock contact angle of water-rock reaction with different temperature and pressure.

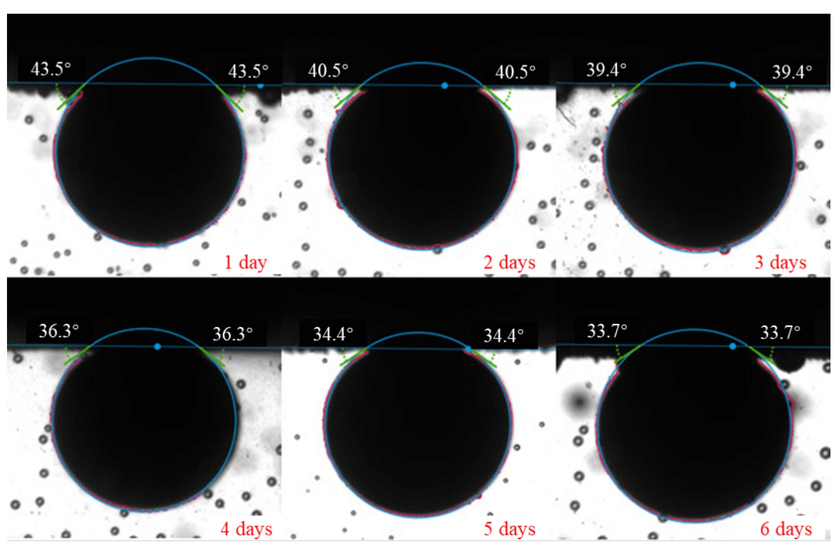


Fig. 8. Variation of contact angle of water-rock reaction with different reaction time.

**Table 3**. Reservoir, rock and fluid characteristics of the model.

| Parameter | Value | Parameter | Value |
|---|---|---|---|
| Reservoir top depth (m) | 250 | Rock compressibility ($kPa^{-1}$) | $3.4\times10^{-6}$ |
| Pay thickness (m) | 45 | Rock heat capacity ($J/m^3\cdot°C$) | $2.5\times10^{6}$ |
| Porosity | 0.35 | Rock thermal expansion coefficient ($°C^{-1}$) | $1.4\times10^{-6}$ |
| Initial temperature (°C) | 20 | Rock thermal conductivity (J/m·day·°C) | $6.64\times10^{4}$ |
| Initial pressure (kPa) | 2,000 | Water heat conductivity (J/m·day·°C) | $5.35\times10^{4}$ |
| Horizontal absolute permeability (mD) | 1,250 | Crude oil thermal conductivity (J/m·day·°C) | $1.15\times10^{4}$ |
| Vertical absolute permeability (mD) | 875 | Gas thermal conductivity (J/m·day·°C) | $0.14\times10^{3}$ |
| Initial oil saturation | 0.7 | Overburden and underburden heat capacity (J/m·day·°C) | $2.1\times10^{6}$ |
| Crude oil compressibility ($kPa^{-1}$) | $7.3\times10^{-7}$ | $CO_2$ molecular weight (kg/mol) | 0.04401 |
| Thermal expansion of crude oil ($°C^{-1}$) | $4.792\times10^{-7}$ | $CO_2$ thermal expansion coefficient ($°C^{-1}$) | $2.8\times10^{-4}$ |

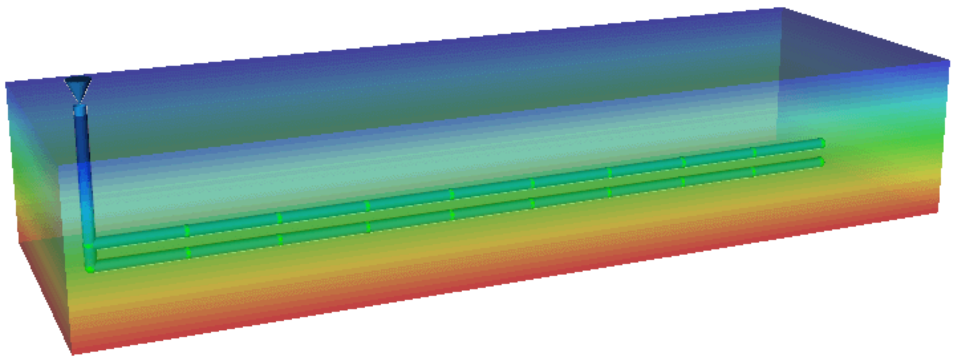

**Fig. 9**. SAGD dual horizontal well perspective model.

voir, rock and fluid property parameters are shown in Table 3. Heavy oil viscosity is based on the oil sample from well PX-2, the viscosity-temperature curve of dehydrated crude oil is shown in Fig. 1.

Length of the injection-production horizontal wells is 460 m, vertical distance between the two wells is 5 m, steam/gas injection well is 40 m from the top of the reservoir. The grid size of the model is 46 m×5 m×1.5 m, and the simulation is carried out using a Cartesian grid (10×19×30) with 5,700 active cells (Fig. 9).

The gas/liquid equilibrium between crude oil, $CO_2$ and water is considered in the model to simulate the dissolution, expansion and viscosity reduction of $CO_2$ in crude oil. According to the phase equilibrium constants calculation formula $K = (KV1/P) \times EXP(KV4/(T - KV5))$ from the CMG user manual, where $KV1$, $KV4$ and $KV5$ correspond to the units of $P$ and $T$. The phase equilibrium constants at the corresponding pressure and temperature are shown in Table 4 (Reid et al., 1977).

**Table 4**. K-Value Coefficients for Selected Components.

| Coefficient | Units | Water | Oil | $CO_2$ |
|---|---|---|---|---|
| $KV1$ | kPa | 1.19E+07 | 1.89E+06 | 8.62E+08 |
| $KV4$ | °C | -3,816.44 | -4,680.46 | -3,103.39 |
| $KV5$ | °C | -227.02 | -132.05 | -272.99 |

### 3.2 SAGD baseline simulation

Under the initial reservoir conditions, crude oil is too viscous to flow. To provide production conditions for the SAGD baseline, preheating is required to achieve thermal communication between the steam injection well and the producing well. Cyclic steam injection stimulation in two wells, three cycles in total. In each cycle, steam injection is 20 days, soak the well 3 days, then production is 30 days. During the preheating cycles, the steam injection temperature is 290 °C and injection rate is 200 $m^3$/d. After preheating, the temperature between the wells reaches about 130 °C and the thermal communication is established (Fig. 10(a)). The average viscosity of oil in the formation between two wells is about 50 mPa·s (Fig. 10(b)), then the production is converted to SAGD baseline.

In SAGD production, the injection steam temperature is 290 °C, with the injection rate of 300 $m^3$/d and the steam quality of 0.8. The characteristics of steam chamber development in different periods during 17 years of SAGD were analyzed. The results indicate that the steam chamber has risen to the bottom of the overburden and started to fall after thirteen years (Fig. 11(a)), more than 3/4 of the reservoir has

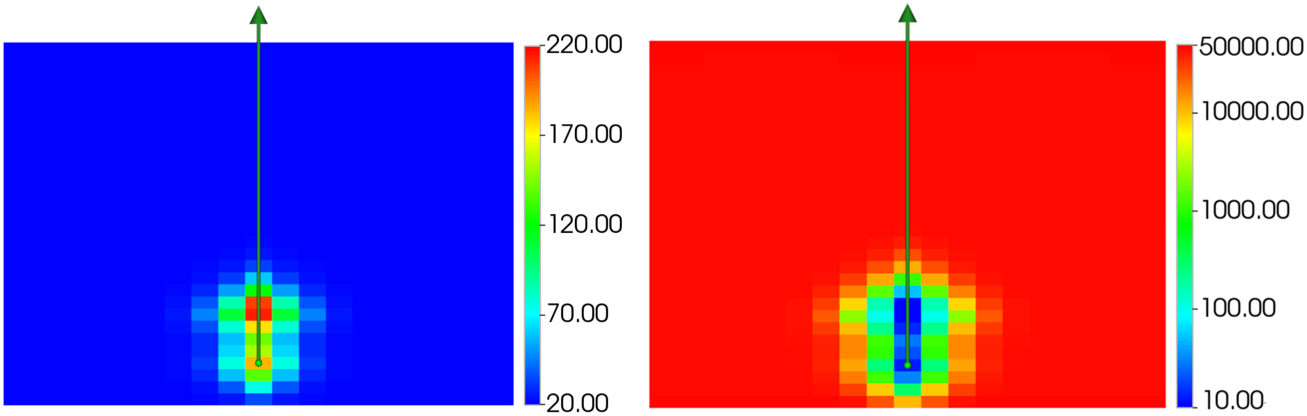


(a) (b)

**Fig. 10**. (a) Temperature profile, and (b) crude oil viscosity profile after preheating.

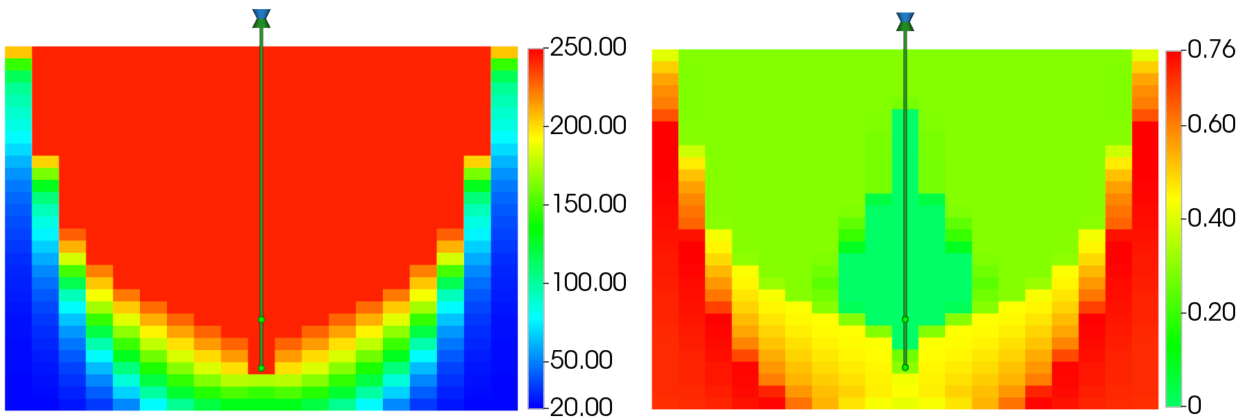


(a) (b)

**Fig. 11**. (a) Temperature profile, and (b) oil saturation profile at 13th year of SAGD.

been heated. Moreover, the oil saturation within 10 m at the top of the reservoir drops to 0.1 (Fig. 11(b)), and it is no longer economical to continue to inject steam into the upper reservoir, therefore, after the 14th year of SAGD production, $CO_2$ is used instead of steam injection. In order to prevent gas channeling in production wells, the gas injection rate is controlled at 5,000 sm$^3$/d (about 90 t/d liquid $CO_2$) and the injection is continuous for 4 years.

### *3.3 Comparisons of SAGD baseline and $CO_2$ injection*

$CO_2$ was injected from the 14th year and continued for 4 years. Comparison the steam chamber development characteristics of the two models shown in Fig. 12, the finally steam chamber temperature of the SAGD baseline is 240–250 °C, another model with the $CO_2$ injection, the average temperature in the steam chamber decreases year by year and finally the temperature in the steam chamber is between 180 and 220 °C, which is high enough for maintaining high flowing capacity of the crude oil.

The energy consumption and heat loss from the two models are compared, with results summarized in Table 5. The SAGD baseline energy consumption from 14$^{th}$ year to end is 757,188$\times$10$^6$ kJ, conversion to the energy consumption per cubic meter of oil production is 13.06$\times$10$^6$ kJ/m$^3$. With a given thermal value of natural gas (35.588$\times$10$^3$ kJ/m$^3$), this equals to the total amount of natural gas consumption of 21.27$\times$10$^6$ m$^3$ or the natural gas consumption per cubic meter of oil production is 366.92 m$^3$. However, the cumulative oil recovery from SAGD baseline is only 2.48% higher than that from $CO_2$ injection case.

Part of the energy consumption in the SAGD Baseline case is used to heat the formation and crude oil, another 16.73% of energy is lost to the surrounding formations. The energy loss in the SAGD baseline case is 1.77 times of that from $CO_2$ injection case. This demonstrates that the accumulation of gas from $CO_2$ injection case provides the insulation to the top formation and reduces heat loss. The simulation results reveal that 7.31$\times$10$^6$ sm$^3$ of $CO_2$ is injected while 2.81$\times$10$^6$ sm$^3$ of $CO_2$ is produced, about 38.4% of the injected $CO_2$ stored in the reservoir (Kong et al., 2021), which is of great significance for reducing carbon emissions and achieving carbon neutrality (Hu et al., 2019).

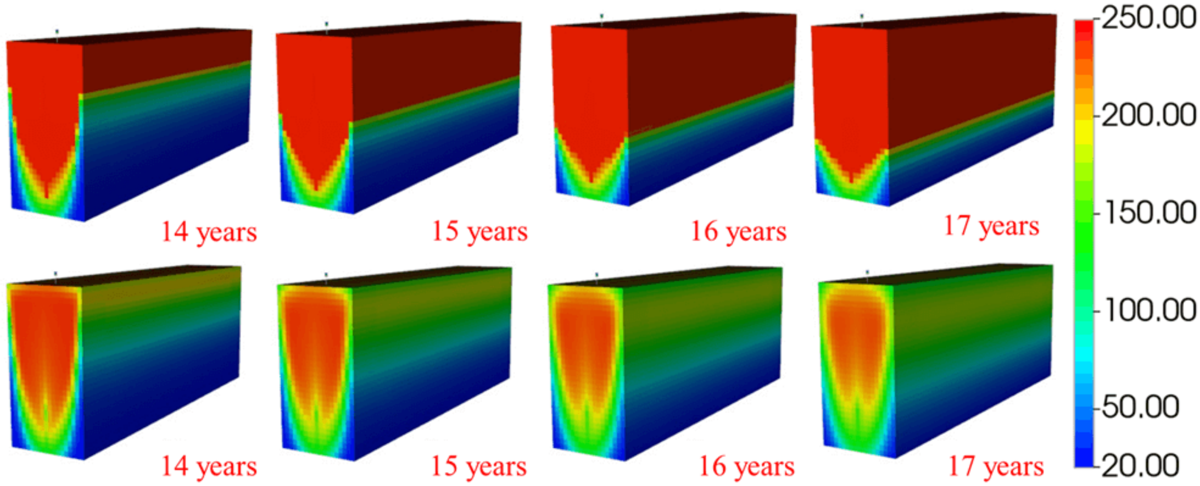


**Fig. 12**. SAGD baseline and $CO_2$ injection steam chamber characteristics.

**Table 5**. SAGD wind-down energy utilization and cumulative oil production.

| Case | Energy injection ($10^6$ kJ) | Energy lost ($10^6$ kJ) | Oil Cumulative ($m^3$) | Energy consumption of unit volume ($10^6$ kJ/$m^3$) | $CO_2$ storage rates (%) |
|---|---|---|---|---|---|
| SAGD Baseline | 757,188 | 126,703 | 57,986 | 13.06 | — |
| $CO_2$ injection | 0 | 71,431 | 46,155 | 0 | 38.4% |

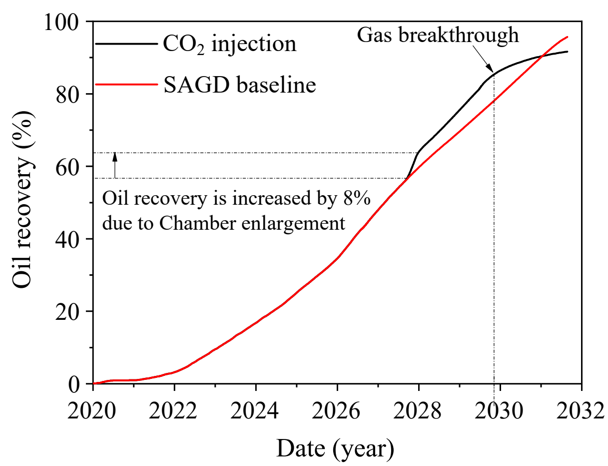


**Fig. 13**. Recovery degree curve of the two models.

It can be seen from Fig. 13 that the steam chamber continues to expand laterally, which increases the recovery factor at the initial stage of $CO_2$ injection by about 6%. Gas channeling occurred about one year after $CO_2$ injection, and the growth rate of recovery became slower. Oil recovery from SAGD baseline is 57.86%, comparing to the oil recovery from $CO_2$ injection is 55.39%, the recovery factor of the two development methods differs by 2.48%. Based on the comparative analysis of the energy consumption from SAGD Baseline case and from $CO_2$ injection cases, and the important social significance of $CO_2$ storage, it is feasible to implement $CO_2$ injection in the SAGD wind-down stage in terms of technical, economic and social benefits. It should be noted that since the flow and diffusion capacity of $CO_2$ are much higher than that of steam or hot water, due to the small well spacing between the injection and production wells in dual-well SAGD well pattern, it is easy to cause gas breakthrough if the $CO_2$ injection rate is not well controlled. Controlling the $CO_2$ injection and production rates is one of the effective methods to delay the gas breakthrough time and improve the $CO_2$ drainage efficiency.

Fig. 14 shows the $CO_2$ mole fraction in oil and gas phases respectively. A ring of high gas concentration is formed around the interface of the steam chamber, which helps to reduced heat loss. The operating pressure of SAGD usually is 2–5 MPa, where $CO_2$ dissolution in the crude oil is limited, and therefore the $CO_2$ molar fraction in the oil phase is between 0 and 2%. Most of the $CO_2$ is distributed as free gas in the upper part of the steam chamber. With the increase of $CO_2$ injection, gas-assisted gravity drainage is enhanced (Watheq and Andrew, 2019). Some $CO_2$ is dissolved in the remaining oil, and the volume expansion of the crude oil can increase the elastic energy of the formation (Figs. 14(a) and 14(b)). At the same time, the expanded remaining oil becomes mobile oil by breaking the constraints from the reservoir pores or formation water, consequently improving the microscopic oil drainage efficiency (Li et al., 2020).

Fig. 14(c) show the crude oil viscosity is reduced to 30–34 mPa·s in the oil-gas transition zone, which is in agreement with the results from the laboratory experiment tests (Table 2). Although the temperature in the steam chamber during $CO_2$ injection is lower than that in SAGD baseline case, the reduction of crude oil viscosity at the oil-gas transition zone facilitates the flow of crude oil at the edge of the steam chamber to the production well, thus compensating for the

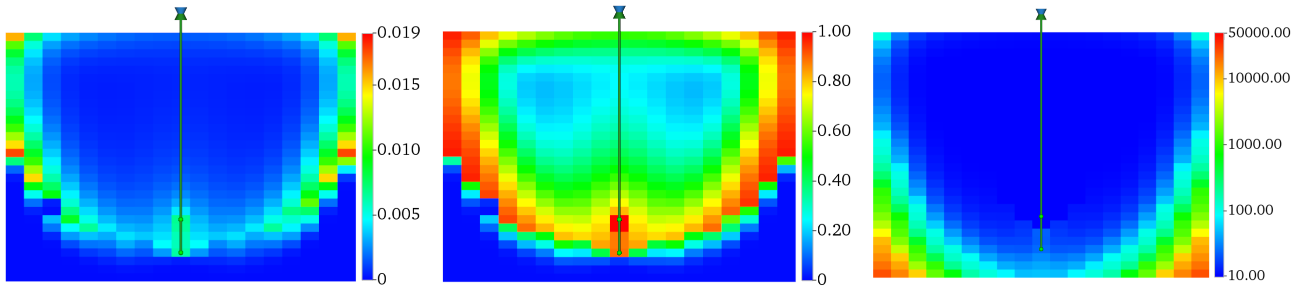


(a) (b) (c)

**Fig. 14**. $CO_2$ molar fractions (a) in oil phase, and (b) in gas phase, and (c) oil viscosity of $CO_2$ injection case (17th year).

influence of temperature reduction on the flow of crude oil. In addition, oil and water are mixed at the steam chamber edge, the emulsification of crude oil tends to increase the emulsion viscosity. The injection of $CO_2$ into the steam chamber has effect on the dehydration and demulsification of crude oil, and the higher the pressure, the better the demulsification effect. After the heavy oil emulsion is dehydrated, the viscosity will decrease, which is beneficial to gravity drainage.

## 4. Conclusions

Based on the above-presented result, the following conclusions reached:

1) $CO_2$ will dissolve and expand with heavy oil, which will reduce the viscosity of heavy oil and increase drainage energy. $CO_2$ also has a demulsification effect, and the higher the dissolution pressure, the larger effect on demulsification. These combined effects can reduce the emulsion viscosity by more than 50% at the highest.
2) The extraction of light hydrocarbons from $CO_2$ can lead to solid phase deposition of waxes and asphaltenes, when the steam chamber temperature reaches 200 °C, the amount of solid phase deposition induced by $CO_2$ extraction is only 0.016 kg/m$^3$.
3) $CO_2$ will change the wettability of the rock surface, making the water-rock reaction temperature and pressure higher, the smaller the contact angle and the stronger the hydrophilicity; the longer the reaction time, the stronger the hydrophilicity. Decreasing the contact angle can reduce the oil phase surface adhesion work, which is facilitate gravity drainage.
4) Undissolved $CO_2$ is distributed in the upper part of the steam chamber, forming a thermal insulation layer and reducing heat loss. Heat loss from traditional SAGD baseline case is 1.77 times that with $CO_2$ injection process, but the recovery factor is only 2.48% higher.
5) Crude viscosity in oil-gas transition zone is reduced to 30–40 mPa·s, which is beneficial for the crude oil flow from the steam chamber interface to the production well, compensating for the influence of reduced temperature from $CO_2$ injection.
6) Under the current operating conditions, 38.4% of the injected $CO_2$ would be stored in the reservoir.

## Acknowledgement

The authors would like to thank CMG Ltd for allowing us access to the STARS simulators. The authors would also like to thank the reviewers and editors whose critical comments were very helpful in preparing this article.

## Conflict of interest

The authors declare no competing interest.



## References

Ali, S. B., Olushola, G. S., Eric, J. M. Performance analysis of SAGD wind-down process with $CO_2$ injection. Paper SPE 113234 Presented at Symposium on Improved Oil Recovery, Tulsa, Oklahoma, 20-23 April, 2008.

Ameri, A., Farajzadeh, R., Shojai, K. N., et al. Effect of matrix wettability $CO_2$ assisted gas-oil garvity drainage in naturally fractured reservoirs. Paper Presented at 77$^{th}$ EAGE Conference and Exhibition, Madrid, Spain, 1-4 June, 2015.

Butler, R. M. The steam and gas push (SAGP). Journal of Canadian Petroleum Technology, 1999, 38(3): 47-54.

Butler, R. M., Stephens, D. J. The gravity drainage of steam-heated heavy oil to parallel horizontal wells. Journal of Canadian Petroleum Technology, 1981, 20(2): 90-96.

Daniel, J. S. Greenhouse gas sources and mitigation strategies from a geosciences perspective. Advances in Geo-Energy Research, 2021, 5(3): 274-285.

Davarpanah, A., Mirshekari, B. Experimental study of $CO_2$ solubility on the oil recovery enhancement of heavy oil reservoirs. Journal of Thermal Analysis and Calorimetry, 2020, 139(2): 1161-1169.

Dong, X., Liu, H., Chen, Z., et al. Enhanced oil recovery techniques for heavy oil and oilsands reservoirs after steam injection. Applied Energy, 2019, 239: 1190-1211.

Ehsan, A., Belenitza, S. D., Sudarshan, R. M., et al. Evaluation of air injection into mature SAGD chambers as a follow up/wind-down strategy, Using a novel large scale 3-D physical model. Paper SPE 196049 Presented at Annual Technical Conference and Exhibition, Calgary, Alberta,

30 September-2 October, 2019.
Fan, Y., Mei, L., Liu, H. Geochemical characteristics and accumulated process of heavy crude oil of Chunguang oilfield in Junggar Basin, China. Journal of Earth Science, 2016, 27: 846–855.
Fang, T., Shi, J., Sun, X., et al. Supercritical $CO_2$ selective extraction inducing wettability alteration of oil reservoir. Journal of Supercritical Fluids, 2016, 113: 10-15.
Gu, F. G., Chan, M., Rismyhr, O., et al. Optimization of SAGD wind-down and blow-down for Athabasca oil sands. Paper SPE 165481 Presented at Heavy Oil Conference-Canada, Calgary, Alberta, 11-13 June, 2013.
He, J., Li, M., Zhou, K., et al. Effects of vugs on resistivity of vuggy carbonate reservoirs. Petroleum Exploration and Development, 2020a, 47(3): 527-535.
He, J., Li, M., Zhou, K., et al. Radial resistivity measurement method for cylindrical core samples. Interpretation, 2020b, 8(4): 1071-1080.
Hosseinpour, M., Hajialirezaei, A. H., Soltani, M., et al. Thermodynamic analysis of in-situ hydrogen from hot compressed water for heavy oil upgrading. International Journal of Hydrogen Energy, 2019, 44(51): 27671-27684.
Hu, Y., Hao, M., Chen, G., et al. Technologies and practice of $CO_2$ flooding and sequestration in China. Petroleum Exploration and Development, 2019, 46(4): 753-766.
Kong, D. B., Gao, Y. B., Hemanta, S., et al. Experimental investigation of immiscible water-alternating-gas injection in ultra-high water-cut stage reservoir. Advances in Geo-Energy Research, 2021, 5(2): 139-152.
Li, N., Tan, X., Ren, Z. Micro-sweep characteristics of $CO_2$ flooding. Chemistry and Technology of Fuels and Oils, 2020, 56(4): 658-664.
Li, S., Yu, T., Li, Z., et al. Experimental investigation of nitrogen-assisted SAGD in heavy-oil reservoirs: A two-dimensional visual analysis. Fuel, 2019, 257: 116013.
Mohammad, J. Steam alternating non-condensable gas injection for more heavy oil recovery. Energy, 2022, 240: 122476.
Reid, R. C., Sherwood, T. K., Prausnitz, J. M. The Properties of Gases and Liquids. New York, USA, McGraw-Hill Education, 1977.
Ren, J., Wang, T., Chen, Y., et al. Research status and application potential of $CO_2$ mineralization. Earth Science, 2020, 45(7): 2413-2425. (in Chinese)
Seyyed, M. S., Mehran, S. Intermittent $CO_2$ and viscosity-reducing gas (VRG) injection for enhanced heavy oil recovery. Fuel Processing Technology, 2017, 164: 1-12.
Song, Z. Y., Zhu, W. Y., Wang, X., et al. 2-D pore-scale experimental investigations of asphaltene deposition and heavy oil recovery by $CO_2$ flooding. Energy & Fuels, 2018, 32(3): 3194-3201.
Wang, F., Mou, Z., Liu, P., et al. Experiment and numerical simulation on mechanism of $CO_2$ assisted mining in super heavy oil reservoirs. Petroleum Geology and Recovery Efficiency, 2017, 24(6): 86-91. (in Chinese)
Wang, H. Y., Torabi, F., Zeng, F. H., et al. Experimental and numerical study of non-equilibrium dissolution and exsolution behavior of $CO_2$ in a heavy oil system utilizing Hele-Shaw-like visual cell. Fuel, 2020, 270: 117501.
Watheq, J. A., Andrew, K. W. Field-scale evaluation of re-injecting the associating produced gas through the GDWS-AGD EOR process. Paper SPE 195470 Presented at Europec featured at 81$^{st}$ EAGE Conference and Exhibition, London, England, 3-6 June, 2019.
Xi, C., Qi, Z., Zhang, Y., et al. $CO_2$ assisted steam flooding in late steam flooding in heavy oil reservoirs. Petroleum Exploration and Development, 2019, 46(6): 1242-1250.
Zanganeh, P., Dashti, H., Ayatollahi, S. Visual investigation and modeling of asphaltene precipitation and deposition during $CO_2$ miscible injection into oil reservoirs. Fuel, 2015, 160: 132-139.
Zhang, Y. J., Shen, D. H., Gao, Y. R., et al. Physical simulation experiments on $CO_2$ injection technology during steam assisted gravity drainage process. Acta Petrolei Sinica, 2014, 35(6): 1147-1152. (in Chinese)
Zhao, L., Law, D. H. S., Coates, R. Numerical study and economic evaluation of SAGD wind-down methods. The Journal of Canadian Petroleum Technology, 2003, 42(1): 53-57.
Zhao, L., Law, D. H. S., Nasr, T. N. SAGD wind-down: Lab test and simulation. The Journal of Canadian Petroleum Technology, 2005, 44(1): 49-53.